High-Responsivity Low-Voltage 28-Gb/s Ge p-i-n Photodetector With Silicon Contacts

Hong Tao Chen, Peter Verheyen, Peter De Heyn, Guy Lepage, Jeroen De Coster, Philippe Absil, Gunther Roelkens, and Joris Van Campenhout

***Abstract*—We report a high-performance germanium waveguide photodetectors (WPDs) without doping in germanium or direct metal contacts on germanium, grown on and contacted through a silicon p-i-n diode structure. Wafer-scale measurements demonstrate high responsivities larger than 1.0 A/W across the C-band and low dark current of ∼3 nA at –1 V and ∼8 nA at –2 V. Owing to its small dimensions, the Ge WPD exhibits a high optoelectrical 3-dB bandwidth of 20 and 27 GHz at low-bias voltages of –1 and –2 V, respectively, which are sufficient for operation at 28 Gb/s. The reduced processing complexity at the tungsten contact plug module combined with the high responsivity makes these Ge WPD devices particularly attractive for emerging low-cost CMOS-Si photonics transceivers**

***Index Terms*—Germanium photodetector, optical interconnects, silicon photonics.**

I. Introduction

GERMANIUM photodetectors are a critical building block in silicon photonics based optical interconnects. They have been extensively researched, and various device structures have been developed [1]–[9]. Waveguide photodetectors are advantageous over surface illuminated photodetectors owing to their ability to create longer absorption lengths without causing a carrier-transit-time limitation to their bandwidth. Waveguide germanium photodetectors based on vertical p-i-n (VPIN) junction configuratio and lateral p-i-n junction configuratio have been demonstrated with typical responsivity around 0.8 A/W and bandwidth high enough for 40 Gb/s operation at 1550 nm wavelength [1]–[6].

However, both types of devices require doped germanium to form the p-i-n junction, as well as direct metal contact on germanium with metal via plugs. Germanium processing received far less research attention compared to silicon, and is therefore much less well understood and characterized. Besides, it is well recognized that absorption due to the metal contacts on germanium and free carrier absorption in the heavily doped contact region are responsible for a substantial responsivity decrease in germanium WPDs. Hence, a germanium photodetector that does not require doping or contacting of germanium is desirable. However, this should not impact device speed: for practical applications, 25 Gb/s or even 40 Gb/s under low-voltage operation are typical requirements. Although [8], [9] have demonstrated photodetectors without doping or contacting of germanium, it requires a high bias voltage of −4 V for the devices to achieve an opto-electrical 3 dB bandwidth of ∼20 GHz, which is necessary for photodetectors to receive 25 Gb/s on–off keying (OOK) signals. The high bias voltage of −4 V is however not CMOS compatible.

In this paper, we report germanium waveguide photodetectors without doping in or metal via-contact on germanium. A lateral P+(Si)-I(Ge)-N+(Si) (LPIN) diode is formed with both anode and cathode contacts on silicon. They are named Si-LPIN photodetectors hereafter. At −1 V, the Si-LPIN photodetectors gives 20 GHz opto-electrical 3 dB bandwidth, and it is enhanced to 27 GHz at −2 V. The devices were measured to have a responsivity higher than 1 A/W at −1 V reverse bias in the wavelength range from 1505 to 1580 nm. The dark current is measured to be 3.3 nA at −1 V and 7.7 nA at −2 V. 28 Gb/s clearly open eye diagrams are demonstrated. Complete experimental data of our baseline (BL) germanium photodetectors based on a VPIN junction are also given for reference.

II. Device Design and Fabrication

The Si-LPIN waveguide photodetectors are implemented in IMEC's fully integrated Si Photonics Platform along with Si modulators [10] and various passive devices. They go through a process fl w described in [11]. The cross section of the Si-LPIN photodetectors is schematically shown in Fig. 1(a). In Fig. 1(b), our BL germanium photodetector based on a VPIN with P-type via-contact on top of germanium and N-type via contact on the silicon underneath is shown for reference. They are referred to as BL-VPIN photodetectors hereafter. It can be seen that, compared to the BL-VPIN photodetectors configuration there is no ion implantation in or metal via-plugs on germanium. The Si-LPIN photodiode shares exactly the same doping levels and contact process module of a silicon modulator. This significantl simplifie the silicon photonics process fl w and will ultimately reduce the cost of building silicon-based photonic integrated circuits.

The electric fiel distribution in Si-LPIN photodetectors and BL-VPIN photodetectors at –1 V obtained by numerically solving Poisson's equation are shown in Fig. 2. In most of the germanium region, the electric fiel is stronger than 10^4 V/cm at

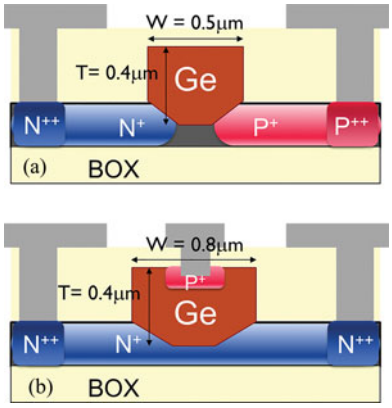

Fig. 1. Schematic cross-section with germanium dimensions of (a) Si-LPIN photodetectors and (b) BL-VPIN photodetectors.

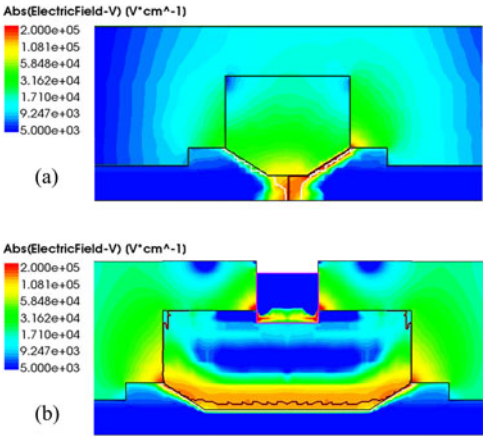

Fig. 2. Electric fiel distribution in (a) Si-LPIN photodetector at –1 V and (b) BL-VPIN photodetector at −1 V.

–1 V reverse bias for Si-LPIN photodetectors. It is strong enough for photo-generated carriers to drift at saturation velocity. The electric fiel is uniform in Si-LPIN photodetectors, while in BL-VPIN photodetectors, the strong electric fiel is confine to the bottom part of the germanium, where much higher defect density is expected due to the 4% lattice mismatch between germanium and silicon. These defects will become active current leakage channels under high electric field Thus, lower dark current can be expected for Si-LPIN photodetectors. In addition, considering there is no via-contact metal absorption and free carrier absorption in the heavy doping contact region, much higher responsivity can be expected for Si-LPIN photodetectors.

III. Device Characteristics

A. Static Measurements

A typical static current-voltage characteristic of a 13.8 μm-long and 0.5 μm-wide Si-LPIN photodetector is shown in Fig. 3. The device has a remarkably low dark current of 3 nA at –1 V. It is still lower than 10 nA as the bias is increased to –3 V. This is among the lowest dark current values that have been reported for Ge WPDs [5]. The photocurrent was measured at 1567 nm

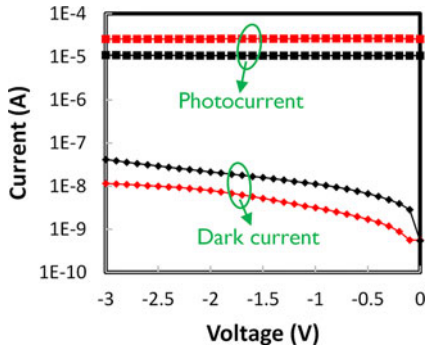

Fig. 3. Current-voltage characteristics of a 13.8 μm-long and 0.5 μm-wide Si-LPIN photodetector (red curves) and a 13.8 μm-long and 0.8 μm-wide BL-VPIN photodetector (black curves).

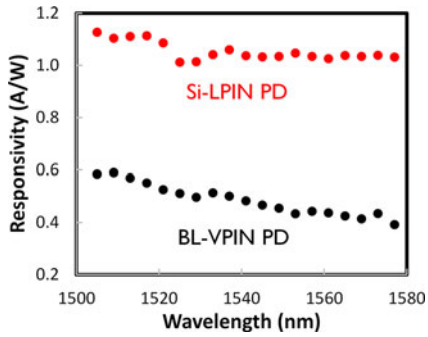

Fig. 4. Responsivity versus wavelength for the Si-LPIN photodetector and the BL-VPIN Ge photodetector.

wavelength with a received optical power of −15.9 dBm. As the bias voltage was increased from 0 to –3 V, the photocurrent was almost constant owing to the relatively strong built-in electric fiel that is capable of sweeping out the majority of photo-generated carriers within their lifetime. The measured responsivity is 1.0 A/W.

The dark current and photocurrent of a 13.8 μm-long and 0.8 μm-wide BL-VPIN photodetector are also shown in Fig. 3 for reference. The photocurrent was measured at the same wavelength and under the same input optical power as that for the Si-LPIN photodetector. It can be seen that the Si-LPIN photodetector is capable of obtaining a photocurrent up to ∼2.5 times higher than that of a BL-VPIN device. At the same time, the dark current is three times lower than that of the latter.

The responsivity in the wavelength range between 1505 and 1580 nm of both devices was further measured and is shown in Fig. 4. The Si-LPIN photodetector has a responsivity higher than 1.0 A/W in the whole wavelength range, which is much higher than that measured from the BL-VPIN device (0.4–0.6 A/W). This is among the best results that have been published for Ge WPDs [2]–[4], [7]–[9].

Wafer-scale dark current data of both the Si-LPIN photodetector and the BL-VPIN photodetector at −1 and −2 V are shown in Fig. 5. The average dark current is 3.3 and 7.7 nA respectively, with a standard deviation of 0.5 and 0.8 nA, at −1 and −2 V. In Fig. 6(a) and (b), contour plots of the wafer-scale responsivity

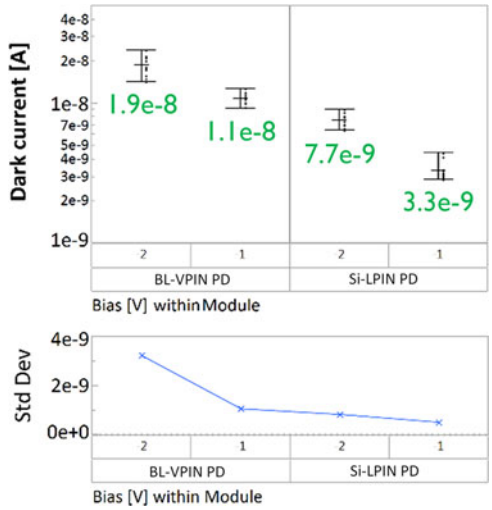

Fig. 5. Wafer-scale dark current data of the Si-LPIN photodetector and the BL-VPIN photodetector at −1 and −2 V. The mean of the wafer-scale data is annotated explicitly in the graph; standard deviations ("std Dev") of the wafer-scale data is given separately.

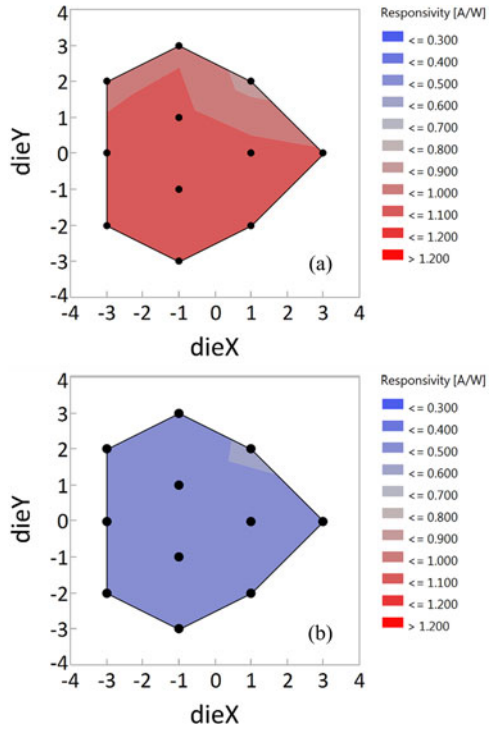

Fig. 6. Wafer-scale responsivity data at 1567 nm for (a) the Si-LPIN photodetector and (b) the BL-VPIN photodetector.

data of both the Si-LPIN photodetector and the BL-VPIN photodetector at ∼1560 nm wavelength are shown. As for reponsivities larger than 0.95 A/W, it shows a yield of 91% for Si-LPIN photodetectors.

B. Small-Signal Measurements

Small-signal radio-frequency (RF) measurements were further carried out to characterize the high-speed performance of

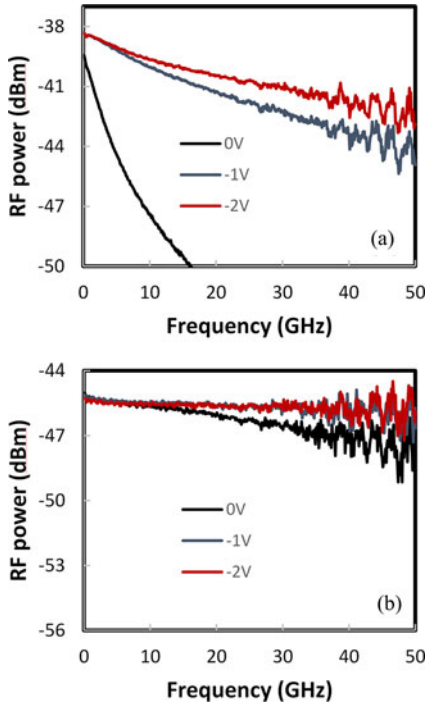

Fig. 7. S21 traces at different bias voltages from small-signal RF measurements for (a) the Si-LPIN photodetector and (b) the BL-VPIN photodetector.

the devices. S_{21} traces at different bias voltages of the Si-LPIN photodetector are shown in Fig. 7(a). At −1 V, the device has a 3 dB bandwidth of 20 GHz, sufficien for receiving 25 Gb/s OOK signals. The low bandwidth of 2.8 GHz at 0 V is due to the long transit time under the relatively low electric fiel strength in the device at 0 V. The bandwidth is further enhanced to 27 GHz as the bias voltage increases to −2 V.

S21 traces of the BL-VPIN photodetector are also shown in Fig. 7(b) for reference. The device has a very high 3 dB bandwidth of 42 GHz at 0 V and up to ∼50 GHz when the bias increases to −1 V. It should be noted that 50 GHz is the upper limit of our equipment measurement range. The wafer-scale 3 dB bandwidth of both devices at 0, −1 and −2 V is shown in Fig. 8. The average 3 dB bandwidth is 20 and 27 GHz at –1 and –2 V respectively for the Si-LPIN photodetector. The BL-VPIN photodetector has a much higher bandwidth of 48 and 49 GHz at −1 and −2 V respectively.

C. Large-Signal Measurements

Next, data transmission experiments were carried out. Light from a 1.55 μm laser was modulated with a 28 Gb/s non-return to zero pseudo random bit sequence ($2^{31}-1$ word length) by an external 44 Gb/s $LiNbO_3$ modulator and detected by the Si-LPIN photodetector and BL-VPIN device. The bias voltage was applied to the photodetector using a 50 GHz RF probe connected to a 40 GHz bias-tee. The photocurrent output was measured with an Agilent oscilloscope with a 60 GHz remote sampling head plug-in. Eye diagrams of the Si-LPIN photodetector at −1 and −2 V are shown in Fig. 9(a) and (b). In Fig. 9(c), the eye diagram of the BL-VPIN photodetector at −1 V is shown for

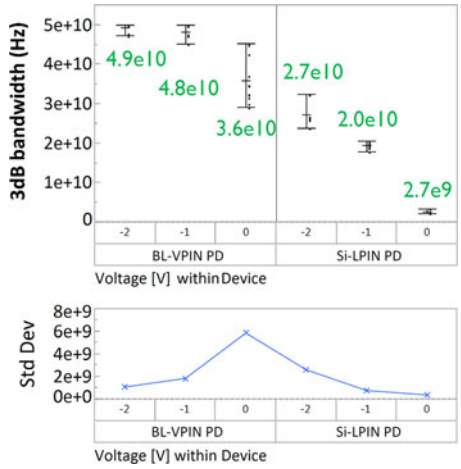

Fig. 8. Wafer-scale opto-electrical 3 dB bandwidth of the Si-LPIN photodetector and the BL-VPIN photodetector at 0, –1 and –2 V. The mean of the wafer-scale data is annotated explicitly in the graph; standard deviations ("std Dev") of the wafer-scale data is given separately.

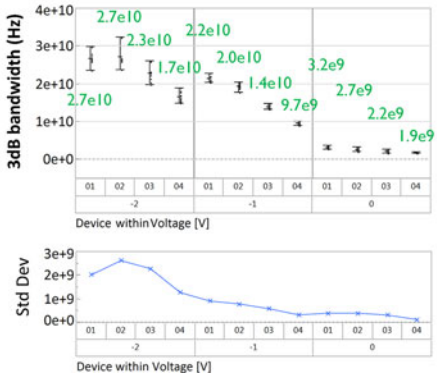

Fig. 10. Wafer-scale opto-electrical 3 dB bandwidth data of four Si-LPIN photodetectors with different germanium width at 0, –1 and –2 V. The width of germanium are 0.4 μm (device 01), 0.5 μm (device 02), 0.6 μm (device 03) and 0.7 μm (device 04). The mean of the wafer-scale data is annotated explicitly in the graph; standard deviations ("std Dev") of wafer-scale data variance are given separately.

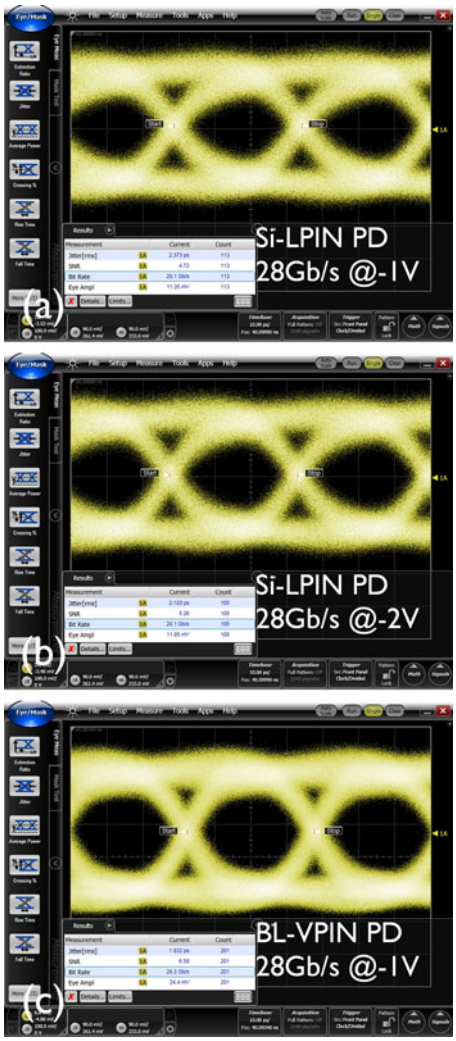

Fig. 9. 28 Gb/s eye diagrams of a Si-LPIN photodetector at (a) –1 and (b) –2 V. (c) 28 Gb/s eye diagram of a BL-VPIN photodetector at –1V.

reference. It can be seen that the rise time and fall time in the eye diagrams of the Si-LPIN photodetector are longer than that in the eye diagram of the BL-VPIN photodetector, limited by the lower opto-electrical bandwidth. The clearly open eyes from the contact-free photodetector with low bias voltage at -1 and -2 V indicate high performance data reception at 28 Gb/s.

IV. Discussion and Outlook

Wafer-scale opto-electrical 3 dB bandwidth data of Si-LPIN photodetectors with different germanium width are shown in Fig. 10. At 0 and -1 V, the narrower the germanium width, the higher the 3-dB bandwidth. Since a quasi-lateral p(Si)-i(Ge)-n(Si) junction is formed in a Si-LPIN photodetector, changes in germanium width implies a change in the intrinsic region width in the p-i-n junction. The shorter carrier transit distance in the narrower devices results in a shorter transit time under the assumption that carriers drift at saturation velocity. The bandwidth is mainly limited by the carrier transit time, which is confirme by the fact that the bandwidth increases as bias is increased. At -2 V, the trend still holds for the last three devices, yet, the bandwidth of the firs device is similar to that of the second device. This is attributed to the increase of the silicon junction capacitance.

It can be seen from Fig. 2(a) that electric fiel strength in the top part of germanium is weaker than that in the bottom. This weak fiel strength is not sufficien ($<1 \times 10^4$ V/cm) for carriers to drift at their saturation velocity. At the same time, the carrier drift distance for carriers generated at the top of the germanium is longer than that at the bottom. Thus, an effective approach to increase the Si-LPIN photodetector bandwidth is to reduce germanium thickness. With stronger electric fiel strength and shorter transit time after adopting thinner germanium, the dependence on narrower germanium to reduce transit time and thus to obtain high bandwidth can be removed. This will eliminate the upper bandwidth limit imposed by the large capacitance of the p-i-n junction formed in silicon.

V. Conclusion

Germanium photodetectors without doping or contacting of germanium were demonstrated with a significantl simplifie fabrication process. At −1 V, the photodetectors give high responsivity, low dark current and relatively high opto-electrical bandwidth, capable of high-performance operation at 28 Gb/s.

References

[1] T. Yin, R. Cohen, M. M. Morse, G. Sarid, Y. Chetrit,D. Rubin, and M. J. Paniccia, "31 GHz Ge n-i-p waveguide photodetectors on Silicon-on-Insulator substrate," *Opt. Exp.*, vol. 15, no. 21, pp. 13965–13971, 2007.

[2] L. Vivien, J. Osmond, J. M. Fédéli, D. Marris-Morini, P. Crozat, J. F. Damlencourt, E. Cassan, Y. Lecunff, and S. Laval, "42 GHz p.i.n Germanium photodetector integrated in a silicon-on-insulator waveguide," *Opt. Exp.*, vol. 17, no. 8, pp. 6252–6257, 2009.

[3] D. Feng, S. Liao, P. Dong, N. Feng, H. Liang, D. Zheng, C. Kung, J. Fong, R. Shafilha J. Cunningham, A. Krishnamoorthy, and M. Asghari, "High-speed Ge photodetector monolithically integrated with large cross-section silicon-on-insulator waveguide," *Appl. Phys. Lett.*, vol. 95, no. 26, pp. 261105–1–261105-3, 2009.

[4] S. Liao, N.-N. Feng, D. Feng, P. Dong, R. Shafiiha C.-C. Kung, H. Liang, W. Qian, Y. Liu, J. Fong, J. E. Cunningham, Y. Luo, and M. Asghari, "36 GHz submicron silicon waveguide germanium photodetector," *Opt. Exp.*, vol. 19, no. 11, pp. 10967–10972, 2011.

[5] C. T. DeRose, D. C. Trotter, W. A. Zortman, A. L. Starbuck, M. Fisher, M. R. Watts, and P. S. Davids, "Ultra compact 45 GHz CMOS compatible Germanium waveguidephotodiode with low dark current," *Opt. Exp.*, vol. 19, no. 25, pp. 24897–24904, 2011.

[6] L. Vivien, A. Polzer, D. Marris-Morini, J. Osmond, J. M. Hartmann, P. Crozat, E. Cassan, C. Kopp, H. Zimmermann, and J. M. Fédéli, "Zero-bias 40Gbit/s germanium waveguide photodetector on silicon," *Opt. Exp.*, vol. 20, no. 2, pp. 1096–1101, 2012.

[7] G. Li, Y. Luo, X. Zheng, G. Masini, A. Mekis, S.Sahni, H. Thacker, J. Yao, I. Shubin, K. Raj, J. E. Cunningham, and A. V. Krishnamoorthy, "Improving CMOS-compatible germanium photodetectors," *Opt. Exp.*, vol. 20, no. 24, pp. 26345–26350, 2012.

[8] T.-Y. Liow, N. Duan, A. E.-J. Lim, X. Tu, M. Yu, and G.-Q. Lo, "Waveguide Ge/Si avalanche photodetector with a unique low-height-profil device structure," presented at the *Opt. Fiber Commun. Conf.*, San Francisco, CA, USA, 2014, Paper M2G.6.

[9] Y. Zhang, S. Yang, Y. Yang, M. Gould, N. Ophir, A. E.-J. Lim, G.-Q. Lo, P. Magill, K. Bergman, T. Baehr-Jones, and M. Hochberg, "A high-responsivity photodetector absent metal-germanium direct contact," *Opt. Exp.*, vol. 22, no. 9, pp. 11367–11375, 2014.

[10] M. Pantouvaki, P. Verheyen, G. Lepage, J. De Coster, H. Yu, P. De Heyn, P. Absil, and J. Van Campenhout, "20Gb/s silicon ring modulator co-integrated with a Ge monitor photodetector," presented at the *Eur. Conf. Opt. Commun.*, London, U.K., 2013, Paper We.3.B.2.

[11] P. Verheyen, M. Pantouvaki, J. Van Campenhout, P. Absil, H. Chen, P. De Heyn, G. Lepage, J. De Coster, P. Dumon, A. Masood, D. Van Thourhout, R. Baets, and W. Bogaerts, "Highly uniform 25 Gb/s Si photonics platform for high-density, low-power WDM optical interconnects," presented at the *Integr. Photon. Res., Silicon Nanophoton. Conf.*, 2014, Paper IW3A.4.

Hong Tao Chen received the master's degree in electronics and communications engineering from the Institute of Semiconductor, Chinese Academy of Sciences, China in 2012. He is currently working toward the Ph.D. degree at Optical I/O Program, Interuniversity Microelectronics Center (IMEC), Leuven, Belgium. He is involved in Photonics Research Group, Ghent University, and IMEC. His research interests include Ge-on-Si-based advanced optical devices for optical interconnection, and his focus is on germanium avalanche photodetectors and germanium p-i-n photodetectors.

Peter Verheyen, biography not available at the time of publication.

Peter De Heyn, biography not available at the time of publication.

Guy Lepage, biography not available at the time of publication.

Jeroen De Coster, biography not available at the time of publication.

Philippe Absil, biography not available at the time of publication.

Gunther Roelkens, biography not available at the time of publication.

Joris Van Campenhout, biography not available at the time of publication.